**Proceedings of the Canadian Society for Mechanical Engineering International Congress 2022**
**CSME Congress 2022**
**June 5-8, 2022, Edmonton, AB, Canada**

# HYDROGEN EMBRITTLEMENT SUSCEPTIBILITY OF Zn-Ni BRUSH PLATING PROCESS

Ashkan Arab[1], Alan Caceres[2], Rajwinder Singh[1], Roger Eybel[2], Mamoun Medraj[1]
[1]Mechanical, Industrial and Aerospace engineering, Concordia University, Montreal, Canada
[2]Safran Landing Systems, Mirabel, Québec, Canada

***Abstract***— Corrosion is one of the most important issues in the aerospace industry and the production of the components of an aircraft. Therefore, certain components of an aircraft are coated in order to provide adequate corrosion protection in service. One of those components is the landing gear of an aircraft which can be protected using either Cadmium or Zn-Ni electroplating. However, one of the major issues associated with this process is the possibility of hydrogen embrittlement (HE) of the base metal. Zn-Ni brush plating is commonly used in aerospace industry for on-site repair of localized coating damage. Thus, in order to evaluate the HE of base metal (SAE 4340 steel) after Zn-Ni brush plating, a 200-hour sustained load test as per ASTM F519 of plated notched specimens was conducted. The results indicate considerable hydrogen embrittlement in the case of non-baked samples while baking even at a temperature of 100°C, which is a significantly lower temperature than the industry standard of 190°C, alleviated the embrittlement. Sand blasting before plating was also found to have a considerable influence in the results of the embrittlement test.

***Keywords; Zn-Ni; Brush plating; Hydrogen embrittlement***

## I. INTRODUCTION

The influence of hydrogen on mechanical properties and the associated HE phenomenon was discovered around the end of the 19th century by Johnson [1] where a significant change in the toughness of iron when immersed in acid was discovered. This change in mechanical properties was attributed to hydrogen and not the acid as he [1] observed that the fracture surface of the embrittled metal releases bubbles. Ever since, extensive research has been carried out to investigate the effects of hydrogen on the mechanical properties [2,3] as well as research into the discovery of the mechanisms involved in this phenomenon. The two most discussed mechanisms in the literature are called Hydrogen Enhanced Localized Plasticity (HELP) and Hydrogen Enhanced Decohesion (HEDE). The HELP mechanism is based on observations by Beachem et al [4] in which the presence of hydrogen induced ductile features on the fracture surface led them to conclude that hydrogen has facilitated dislocation movement. Birnbaum et al [5] also provided further evidence of this phenomenon using TEM observations where the introduction of hydrogen into the specimen increased dislocation velocity while the removal of hydrogen reversed this effect. The HEDE mechanism on the other hand, is based on the notion that the presence of hydrogen reduces the cohesion of the structure across cubic cleavage planes and grain boundaries as well as reducing the strength of interatomic bonds leading to a tensile separation of atoms [6].

It is also important to note that the plasticity effect of hydrogen in the material is not just limited to the HELP mechanism and could manifest itself in other mechanisms discussed in the literature such as hydrogen-enhanced strain-induced vacancy (HESIV) and adsorption- induced dislocation emission (AIDE). The HESIV mechanism is based on the notion that the presence of hydrogen increases the formation and clustering of strain induced vacancies while the AIDE mechanism stipulates that the absorption of hydrogen facilitates both the nucleation and the subsequent movement of the dislocation away from the crack tip and shows itself in the form of shallow dimples [7]. It is also reported in the literature [8-10] that hydrogen can create contradictory characteristics including the presence of dislocation mobility and dislocation pinning at the same time. The two mechanisms of HELP and HEDE can also have interplay and synergy with one another [11].

In the aerospace industry, corrosion is an important issue and aircraft parts such as landing gears require adequate protection against corrosion. One of the ways to provide this protection is to apply a protective coating through electroplating. However, electroplating will in turn expose the part to HE as the presence of hydrogen in the process is unavoidable. HE could prove very fatal given that aircraft parts made from high strength steel are very susceptible to it [12,13]. Hydrogen could dissolve in interstitial atomic sites or find itself trapped in grain boundaries or structural defects [14]. Thus in industry, electroplated parts are subjected to a baking process where they are heated to 190°C for a duration of 24 h no later than 4 h after the end of the plating process [15]. It should also be noted that there are issues other than HE related to electroplating. One such issue is the environmental impact of electroplating. One prominent

example is the fact that one of the most common electroplating processes in the industry; Cd plating; is very toxic given that Cd is a carcinogen [16]. Thus, it is necessary to find a replacement for it. Zn-Ni coatings are one of those replacements which have shown to have a good response to baking [17] as well as superior corrosion protection for steel [18]. The overall properties of the coating however, are dependant on temperature, plating current density, electrodeposition potential and pH [19, 20]. Miura et al [21] reported that optimum properties can be acquired when Nickel content is between 10-15wt% .

Besides, it is important to take the microstructure of the coating as well as the presence of defects into consideration as they will definitely facilitate hydrogen permeation into the coating and impact the effectiveness of the baking process. Rajagopalan et al [22] investigated this very topic as they compared and characterized Zn, Zn-Ni, Cd and Cd-Ti coatings. Figures 1a and 1b show the surface morphologies of Zn-Ni coatings that were deposited at current densities of 48 mA/cm$^2$ and 30 mA/cm$^2$ respectively.

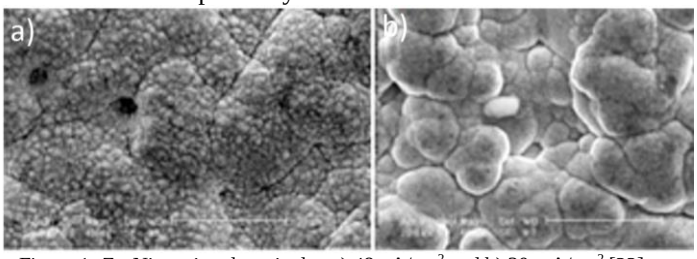


Figure 1- Zn-Ni coating deposited at a) 48mA/cm$^2$ and b) 30 mA/cm$^2$ [22]

The morphologies were evidently different as the coating that was plated at 48 mA/cm$^2$ had visibely smaller platelets of around 1 µm while the one coated at 30 mA/cm$^2$ had platelets ranging from 5-10 µm. Both coatings also had intermittent porosity and micro-cracks. Hydrogen permeability of these coatings was also studied using a Devanathan-Stachurski cell [22]. Figure 2 shows that the coating done at 30 mA/cm$^2$ permeating more hydrogen.

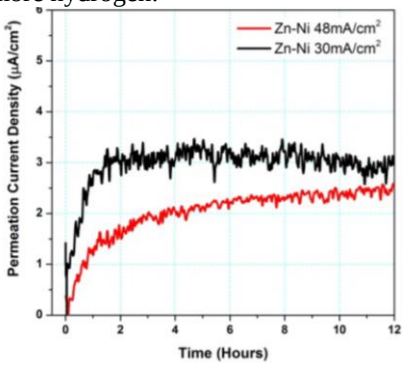


Figure 2- Hydrogen permeation transient for the two Zn-Ni coatings [22]

The importance of micro-cracks and defects were also analyzed by Rajagopalan et al [23] in a similar research. Figure 3 illustrates the diffusion tendecies of hydrogen in a uniform coating compared with a discontinuous coating with micro-cracks and defects. The permeation rate in the discontinouos coating is many orders of magnitude higher compard to the uniform coating and also reaches its plateau faster. The ease of hydrogen diffusion could be a positive or a negative characteristic depending on the circumstances as it may facilitate significant hydrogen diffusion into the sample during plating or it may allow hydrogen to easily leave the sample during the baking process.

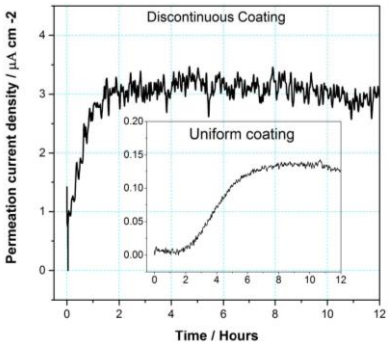


Figure 3- Permeation current densities of uniform and discontinuous Zn-Ni coatings [23]

Table 1 quantifies the results of the permeation test for Zn-Ni coating and the same Zn-Ni coating with micro-cracks to demonstrate the differences more clearly.

Table 1- Hydrogen diffusion tendencies of Zn-Ni coatings with and without microcracks [23]

| **Material** | **Diffusion Coefficient D x 10 $^{-8}$ (cm $^{-2}$ s $^{-1}$)** | **Permeation flux $J_{ss}$ x 10 $^{-11}$(mol s $^{-1}$ cm $^{-2}$)** |
|---|---|---|
| Zn-Ni | 0.391 | 0.087 |
| Zn-Ni with microcracks | 5.778 | 3.177 |

## II. EXPERIMENTAL PROCEDURE

### *A. Sample preparation*

The tests to evaluate HE were conducted in accordance with ASTM F519 [24]. The material used is air melted SAE 4340 steel per AMS 6415 whose composition corresponded to table 2.

Table 2- Composition of SAE 4340 steel

| Element | C | Mn | P | S | Si | Cu | Ni | Cr |
|---|---|---|---|---|---|---|---|---|
| Content (%) | 0.4 | 0.72 | 0.02 | 0.023 | 0.27 | 0.17 | 1.67 | 0.77 |

The material was austenitized in a vacuum furnace at a temperature 829°C for 60 min then subsequently quenched in oil. Afterwards, it was double tempered at 232°C for 4 h each. The mechanical properties of heat treated SAE 4340 are listed in Table 3.

Table 3- Mechanical properties of the 4340 steel after heat treatment

| Mechanical Properties | Value |
|---|---|
| Hardness | 52 HRC |
| Tensile Strength | 1865 MPa |
| Yield Strength | 1558 MPa |
| Elongation | 13% |
| Reduction of Area | 48% |

Subsequently, the raw material was machined in order to prepare small notched bar samples corresponding to the type 1a.1 sample type of ASTM F519 as shown in Figure 4. The samples were subsequently stress relieved at a temperature of 190°C for 4 h after machining.

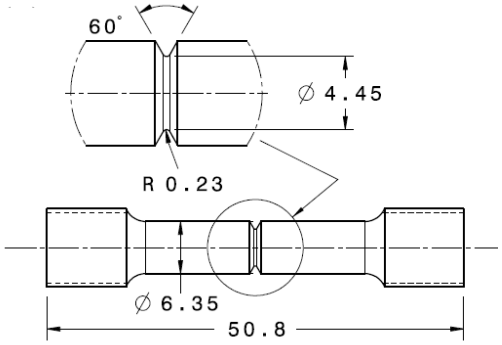


Figure 4- Dimensions of the type 1a.1 sample in millimeters

### *B. Plating Procedure*

Zn-Ni brush plating was used in this work. Brush plating is a quick plating process in which a portable setup consisting of a rectifier, a brush (which is connected to the anode) and a plating solution are used instead of a plating bath which makes the process ideal for in service repairs. Figure 5 illustrates the necessary apparatus for the brush plating process.

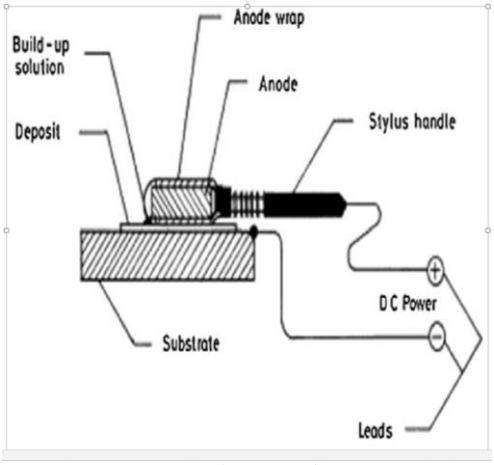


Figure 5- A layout of the setup for brush plating

Three sets of experiments are discussed in this paper where three different parameters were altered during Zn-Ni brush plating process and their resulting effects on the HE of the base metal were observed. These three sets of experiments are performed to:

1. evaluate the effect of change in the baking parameters
2. analyze the effect of skipping the pre-plating sandblasting and
3. analyze the effect of change in plating current density

In the case of experiments 1 and 2, plating was done at a constant voltage of 10 V and continued until a coating of around 10 µm is deposited. For experiments 1 and 3, pre-plating sandblasting was done using an automated setup at a constant pressure of 0.172 MPa (25 psi) and a distance of 35 cm from the samples to ensure a uniform sandblasting and for experiment 2, sandblasting was skipped and baking was not done either. For experiment 3, the current density was fixed instead of the voltage but the coating thickness was the same as the other two experiments. The solution used was an alkaline solution supplied by SIFCO ASC containing $ZnSO_4$ and 16% $NiSO_4$. The samples were attached to a rotating device which was connected to the cathode of the rectifier and the speed of rotation was 60 rpm in order to deposit as uniform a coating as possible. The thickness and the Nickel content of the deposited coating were also measured using an X-ray fluorescence (XRF) gun.

### *C. Embrittlement Test*

The embrittlement test is a sustained tensile load test (SLT) in which a batch of 4 notched samples are attached to each other via couplings and subsequently subjected to a 200 hour tensile load that corresponds to 75% of the fracture strength of the notched samples. Figure 6 represents the layout of the test setup. The notch fracture strength (NFS) of the samples was measured to be 38.59 kN (average of 10 tests). Therefore, the test load was 28.94 kN corresponding to 75% of the NFS. The evaluation of the SLT test results is done as follows:

1- If none of the 4 samples broke within the 200-hour test, the samples were considered to be non-embrittled

2- If one of the samples broke during the 200-hour test, the three remaining samples were subjected to a step load test in which the tensile load was increased from 75% to 90% of the NFS in 5% increments that lasted 2 h each. If the three samples survived this test, they were considered non-embrittled

3- The fracture of two or more samples within the 200-hour test indicated embrittlement

Further, the surface of the fractured samples was analyzed using a Hitachi S-3400N Scanning Electron Microscope (SEM) in order to observe the important features of the fracture surface along with the changes that may occur throughout the surface. The samples were cleaned using acetone in an ultrasonic cleaner before the SEM secondary electron and backscattered analyses.

This work is sponsored by Safran Landing Systems and the Natural Sciences and Engineering Research Council of Canada (NSERC)

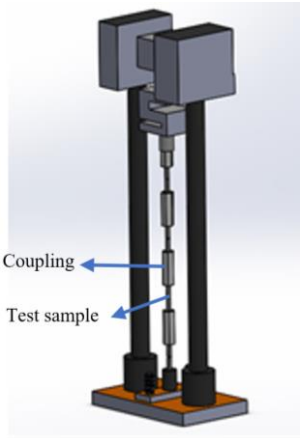


Figure 6- Illustration of a batch of samples attached to each other and placed in the sustained load test setup

## III. RESULTS AND DISCUSSION

The results of the 200-hour sustained load test indicated considerable embrittlement of the samples when they were not baked. Table 4 shows the results of the embrittlement test of 4 batches of samples that underwent different baking procedures. For the non-baked batch, the two fractures occurred within mere 11 h demonstrating significant embrittlement of the samples. On the other hand, baking the samples within 3 h of plating in accordance with industry standards completely relieved embrittlement and all the samples passed the test. Delaying the baking operation by 24 h does not seem to have reduced baking effectiveness as all samples in the third test did not show embrittlement either. However, it is important to note that baking at a high temperature of 190ºC may not necessarily be possible and given that brush plating is usually used for repair purposes, baking at 190ºC might damage the paint that already exists on the part. However, baking at a much lower temperature of 100ºC is also effective at relieving embrittlement. This could prove useful since most painting will be able to withstand the temperature of 100ºC rather than the much higher 190ºC

Table 4- Embrittlement test results of the samples baked under different conditions

| Test # | Test conditions | 200-hour test result | First Fracture (h) | Second Fracture (h) |
|---|---|---|---|---|
| 1 | Zn-Ni non baked | Fail | 5 | 11 |
| 2 | Zn-Ni baked within 3 h | Pass | - | - |
| 3 | Zn-Ni baked after 24 h | Pass | - | - |
| 4 | Zn-Ni baked at 100°C | Pass | - | - |

Another interesting observation is the effect that sandblasting has on the embrittlement of the samples. It appears that without sandblasting, samples show better resistance to embrittlement as they survived for 75 h compared to sandblasted samples which did not endure more than 11 h of the test. The results are summarized in Table 5 and compared with test 1 where samples were sandblasted.

Table 5- Comparison of the test results of the sandblasted samples and those without sandblasting

| Test # | Test conditions | 200-hour test result | First Fracture (h) | Second Fracture (h) |
|---|---|---|---|---|
| 1 | Zn-Ni non baked | Fail | 5 | 11 |
| 5 | Zn-Ni plated without sandblasting and baking | Fail | 32 | 75 |

The noticeable improvement in the test results could be attributed to the absence of alumina residue that could be left over from sandblasting. Figure 7 shows an SEM image taken from the notch of one of the samples after the sandblasting process and it appears that sandblasting with the aforementioned pressure and distance has left small residual alumina particles on the sample (the black particles in Figure 7). Although the issue of embrittlement continues to exist without sandblasting, it seems the residues of sandblasting considerably worsen embrittlement susceptibility. Thus, it is essential to optimize sandblasting parameters to reduce alumina residue as much as possible.

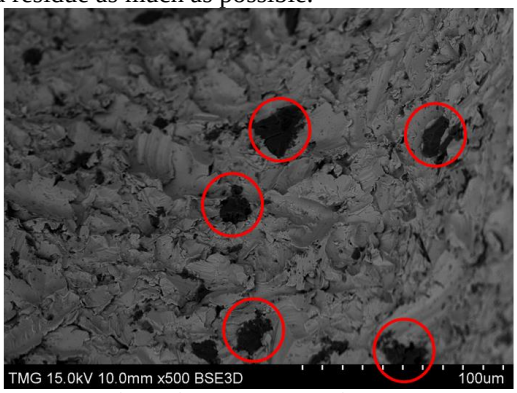


Figure 7- The notch of one of the test samples after sandblasting with visible alumina particles

Figure 8 shows the SEM analysis of the fracture surface of one of the embrittled samples in test 1. The analysis revealed that the surface of the embrittled non-baked samples had visible lines and patterns pointing towards a specific location at the edge of the surface (Figure 8(a)). Upon focusing on that area, an intergranular fracture zone was revealed (Figure 8(b)). The presence of intergranular features is an indication of grain boundary decohesion and a manifestation of the HEDE mechanism. This intergranular region can be assumed to have been the crack initiation point and intergranular fracture appeared nowhere else on the fracture surface (neither on the edges nor in the center). However, away from the crack initiation point, the intergranular features begin to fade away and some ductile features such as surface dimples become more visible (Figure 8(c)). Beyond a certain distance from the fracture initiation point, no sign of intergranular fracture can be seen (Figure 8(d)). However, the existence of these ductile features and the absence of intergranular fracture do not

necessarily indicate the absence of hydrogen influence since it is known that hydrogen could induce plasticity through various mechanisms as discussed in section I. The fracture surfaces of the other embrittled samples also showed similar characteristics.

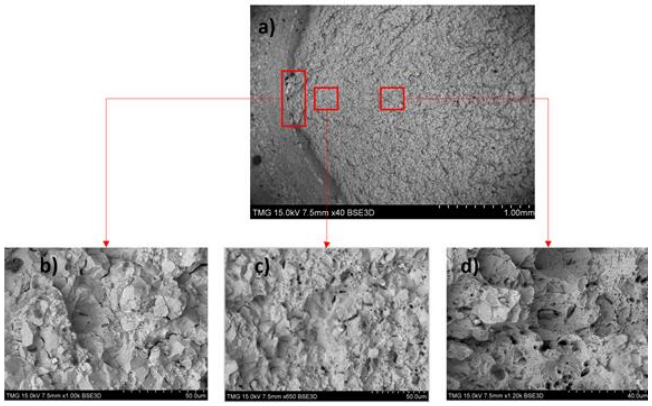


Figure 8- a) Low magnification image of a typical embrittled fracture surface b) the purely intergranular zone near the edge of the notch c) mixed fracture and transition away from intergranular fracture d) centre of the fracture surface with no signs of intergranular fracture

The results of the experiments in which the current was fixed are shown in Table 6.

Table 6- Results of the sustained load test for the samples plated at four different currents

| Test # | Test conditions | 200-hour test result | First Fracture (hr) | Second Fracture (hr) |
|---|---|---|---|---|
| 1 | Zn-Ni plated at 0.66 A/cm$^2$ | Fail | 5 | 8 |
| 2 | Zn-Ni plated at 2 A/cm$^2$ | Fail | 3 | 6 |
| 3 | Zn-Ni plated at 3.3 A/cm$^2$ | Fail | 6 | 6 |
| 4 | Zn-Ni plated at 5.3 A/cm$^2$ | Fail | 4 | 9 |

Surprisingly, carrying out the plating at different fixed currents densities did not change the results of the embrittlement tests. All the experiments failed in a similar manner to the samples of test 1. However, one interesting observation is the change in the coating morphology with the variation in plating current density as compared in Figure 9. The coating morphology largely resembles platelets quite similar to the morphology of the coating reported by Rajagopalan et al [22]. In the case of the samples plated at 0.66 A/cm$^2$ (Figure 9a), the morphology was quite different and did not show the same platelet-like structure of the three other coatings. The platelets also visibly became smaller with increase in plating current density. However, the other feature that is noticeable in all of the coatings is the existence of discontinuity and gaps between the platelets. Through thickness micro-cracks also exist in the coatings as can be seen from Figure 10. These characteristics of the coating morphology will certainly facilitate hydrogen diffusion and might explain why embrittlement is so severe for the samples that are not baked but the samples that are baked even at a lower temperature or after a delay of 24 h show a complete recovery from embrittlement

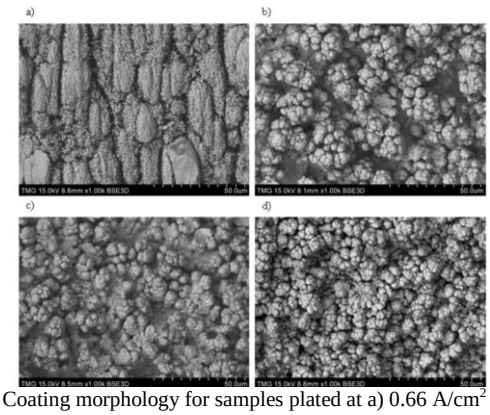


Figure 9- Coating morphology for samples plated at a) 0.66 A/cm$^2$ b) 2 A/cm$^2$ c) 3.3 A/cm$^2$ and d) 5.3 A/cm$^2$.

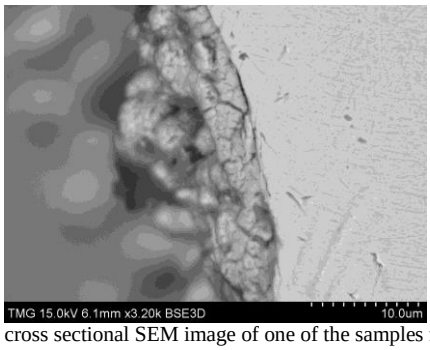


Figure 10- cross sectional SEM image of one of the samples from test 2 showing the coating with visible micro-cracks and crevices

## IV. CONCLUSIONS

The Zn-Ni brush plating process studied in this work caused considerable embrittlement to 4340 steel. However, baking within the time limit of industry standards as well as baking with a delay of 24 h managed to relieve embrittlement. Interestingly, baking at a considerably lower temperature of 100ºC compared to the industry standard of 190ºC also relieved embrittlement. Another important finding is the fact that sandblasting aggravated hydrogen embrittlement which could be the result of the residual alumina particles left on the sample after sandblasting. The sustained load test that was carried out on samples without sandblasting continued for 75 h before the failure of the second sample while for the sandblasted samples, their second failure occurred no longer than 11 h. Of course, additional tests can be conducted to further evaluate the influence of sandblasting and ensure their reproducibility. The observation of the fracture surface of the embrittled samples also revealed an interesting phenomenon in which cracks initiated only in one specific zone at the edge of the fracture surface and intergranular fracture was observed only in that region. The rest of the fracture surface appeared ductile with visible dimples. The morphology of the coating consisted of agglomerations of platelets except for the samples that were coated at a relatively low current density of 0.66 amperes/cm$^2$. There were also noticeable gaps between these platelets as well as the existence of micro-cracks through the thickness of the coating which may have allowed an easier diffusion of hydrogen into the sample.

## REFERENCES


[1] W.H. Johnson, "On the remarkable changes produced in iron and steel by the action of hydrogen and acids," Proc. Royal Society of London, Vol 23, pp.168 – 180, 1874

[2] I.M Robertson, H.K Birnbaum, P. Sofronis, "Hydrogen effects on plasticity,, in Dislocations in solids, Vol 15, J.P Hirth and L.Kubin Eds. Elsevier, 2009, pp.249–293

[3] N.R Moody, S.L Robinson, W.M.J Garrison, "Hydrogen effects on the properties and fracture modes of iron-based alloys," Res Mech , Vol 30, pp.143–206, 1990

[4] C.D. Beachem, "A new model for hydrogen assisted cracking (Hydrogen embrittlement)," Metall Trans, Vol 3, pp. 437 – 451, 1972

[5] H.K. Birnbaum, "Mechanisms of hydrogen related fracture of metals," in Hydrogen effects on materials behavior, N.R. Moody and A.W Thompson Eds. The Minerals, Metals and Materials Society, 1990, pp. 639 – 658

[6] R.A. Oriani, "A mechanistic theory of hydrogen embrittlement of steels," Phys Chem Chem Phys, Vol 76, pp.848 – 857, 1972

[7] S.P Lynch, "Hydrogen embrittlement phenomena and mechanisms," Corros Rev, Vol 30, pp.105–123, 2012

[8] Y. Murakami, T. Kanezaki, Y. Mine, "Hydrogen effect against hydrogen embrittlement," Metall Mater Trans A; Vol 41(10), pp.2548–2562, 2010

[9] Y. Zhao, M.Y. Seok, I.C. Choi, Y.H. Lee, S.J. Park, U. Ramamurty, J.Y. Suh, J.I. Jang "The role of hydrogen in hardening/softening steel: Influence of the charging process," Scr Mater; Vol 107, pp.46–49, 2015

[10] S.Taketomi, R. Matsumoto, S. Hagihara, "Molecular statics simulation of the effect of hydrogen concentration on {112}<111>edge dislocation mobility in alpha iron," ISIJ Int, Vol 57, pp.2058–2064, 2017

[11] P. Novak, R. Yuan, B.P Somerday, P. Sofronis, R.O. Ritchie, "A statistical, physical-based, micro-mechanical model of hydrogen-induced intergranular fracture in steel," J Mech Phys Solids, Vol 58(2), pp.206-226, 2010

[12] L. W. Tsay, M. Y. Chi, Y. F. Wu, J. K. Wu, and D. Y. Lin, "Hydrogen embrittlement susceptibility and permeability of two ultra-high strength steels," Corros Sci , Vol 48, pp.1926-1938, 2006

[13] T. Das, S. Rajagopalan, S.V Brahimi, X. Wang. "A study on the susceptibility of high strength tempered martensite steels to hydrogen embrittlement (HE) based on incremental step load (ISL) testing methodology," Mater Sci Eng A, Vol 716, pp.189–207, 2018

[14] J.P Hirth, "Effects of hydrogen on the properties of iron and steel," Metall Mater Trans A; Vol 11, pp.861–890, 1980

[15] "Plating, cadmium (electrodeposited)," SAE International AMS Standard AMSQQP416D , 2016

[16] M.P. Waalkes, "Cadmium carcinogenesis in review," J Inorg Biochem, Vol 79, pp.241–244, 2000

[17] S. Brahimi, S. Rajagopalan, S.Yue, J.A.Szpunar "Effect of Surface Processing Variables on Hydrogen Embrittlement of Steel Fasteners Part 1: Hot Dip Galvanizing," Can Metall Q, Vol 48(3), pp.293-301, 2009

[18] K.R. Sriraman, S. Brahimi, J.A. Szpunar, J.H. Osborne, S. Yue "Characterization of corrosion resistance of electroposited Zn–Ni, Zn and Cd coatings," Electrochim Acta, Vol 105 , pp.314-323, 2013

[19] G. Barceló, E. García, M. Sarret, C. Müller, J. Pregonas, "Characterization of zinc–nickel alloys obtained from an industrial chloride bath," J Appl Electrochem, Vol 28, pp.1113–1120, 1998

[20] H. Ashassi-Sorkhabi, A. Hagrah, Parvini-Ahmadi, J. Manzoori, "Zinc-Nickel Alloy Coatings Electrodeposited from a Chloride Bath Using Direct and Pulse Current," Surf Coat Technol, Vol 140, pp.278-283, 2001

[21] N. Miura, T. Saito, T. Kanamaru, Y. Shindo, Y. Kitazawa, "Development of New Corrosion-resistant Steel Sheets for Automobiles," Trans Iron Steel Inst Jpn., Vol. 23, pp.913-922, 1966

[22] S. Rajagopalan, S. Brahimi, S. Yue,"Characterization of Hydrogen Permeability in Zn, Zn-Ni, Cd and Cd-Ti Coated Steel.," In International Hydrogen Conference (IHC 2012): Hydrogen-Materials Interactions. B.P Somerday, P.Sofronis Eds. ASME Press, 2014

[23] S. Rajagopalan, S. Brahimi, J. Szpunar, S. Yue, "Hydrogen embrittlement of Zn-, Zn–Ni-, and Cd-coated high strength steel," J Appl Electrochem, Vol 43, pp 441-451, 2013

[24] "ASTM F519: Standard Test Method for Mechanical Hydrogen Embrittlement Evaluation of Plating/Coating Processes and Service Environments,", West Conshohocken, PA, USA, ASTM International, 2018